https://doi.org/10.5194/mr-2026-8
Preprint. Discussion started: 1 June 2026
© Author(s) 2026. CC BY 4.0 License.

Open Access MAGNETIC RESONANCE Discussions

Comparing Fourier Transform and Direct Wave Fitting in NMR FID Data Analysis

Jixin Chen

Department of Chemistry and Biochemistry, Nanoscale & Quantum Phenomena Institute, Ohio University, Athens, Ohio 45701, United States

Correspondence to: Jixin Chen (chenj@ohio.edu)

Abstract. This report compares various simulation and data analysis methods for free induction decay (FID) signals in Nuclear Magnetic Resonance (NMR) Spectroscopy. The methods discussed include discrete fast Fourier transformation (FFT), least squares fitting (LSF), short-time Fourier transformation (STFT), and wavelet transformation. NMR is a widely used technique for elucidating the chemical composition and structure of molecules. It measures the nuclear magnetic spin frequencies of different atoms in a sample, producing signals that are waves over the time domain. This report employs Gaussian wave frequency simulations to model the interference and dephasing among adjacent frequencies of each Gaussian chemical shift. Typically, FIDs are analysed using the FFT algorithm, although least squares fitting and machine learning algorithms are also employed. The simulations indicate that STFT can generate spectrograms that are useful for further neural network training, while LSF is effective in processing signals around or even below one wave cycle.

1 Introduction

Nuclear magnetic resonance (NMR) is widely used in chemistry, materials science, and life science. Solid-state NMR is one of the major spectroscopies used in surface chemistry and catalysis.(Hamers et al., 2017; Weidkamp et al., 2004; Zhang et al., 2014) NMR's free induction decay (FID) signals are sampled in the time domain and are usually analyzed by the fast Fourier transformation (FFT) method.(Hagaman et al., 1997; Esvan and Zeinyeh, 2020; van Beek, 2007; Orekhov et al., 2023; Stern et al., 2007; Hirakawa et al., 2019; Hulse, 2023) It converts the discrete signal collected with fixed time intervals from the time domain to the more intuitive frequency domain signal.(Esvan and Zeinyeh, 2020; Kalstabakken and Harned, 2013; Orekhov et al., 2023) This analysis is done either manually or automatically.(van Beek, 2007; Esvan and Zeinyeh, 2020; Hulse, 2023; Wu et al., 2024) These frequency signals are then correlated with the chemical environment of the atomic nucleus of interest to provide structural information about the molecules. The analysis often averages the dephasing signal of the decaying rotation of the atomic magnetization vectors. Because different atoms decay/damp differently and have different peak-broadening mechanisms, it is often difficult to correlate with the true amplitude of the signal that is proportional to the concentration of the corresponding atom. The traditional method is to simulate the chemical shifts using quantum calculations and then assign the peak intensities and shifts to different signals with a guessed molecular structure.(Bothner-By and Naar-Colin, 1962)

https://doi.org/10.5194/mr-2026-8
Preprint. Discussion started: 1 June 2026
© Author(s) 2026. CC BY 4.0 License.

Open Access MAGNETIC RESONANCE Discussions

Advanced 2D NMR techniques such as COSY and DOSY have been developed to obtain time-evolved information.(Hagaman et al., 1997; Nicolay et al., 2001; Sacristán-Martín et al., 2025)

An alternative analysis method is to directly fit the FID signal using a combination of damping wave functions, such as least squares fitting (LSF) methods.(Castellano and Bothner-By, 1964; Montigny et al., 1990; Nishiyama and Mita, 1989; Vanhuffel et al., 1994) Least squares gradient descent methods such as Newton-Gauss, and the Levenberg–Marquardt algorithm have been used to fit NMR FID data. This approach provides more information than FFT in obtaining phase information, decay lifetime, and initial amplitude. The initial amplitudes and peak areas are particularly useful to correctly quantify the atomic concentrations, and the decay lifetime helps find correlations between atoms, complementary to the traditional quantum simulation-assisted analysis and 2D NMR methods. We recently developed a jump-chain fitting algorithm (JCFIT) that has shown some advantages in fitting damping wave functions compared to gradient descent methods.(Chen, 2024b) It searches exponentially apart from the original guesses of the parameters and skips the gradient calculation, thus making it more robust to the large number of local minima of a wave fitting project.

Artificial neural networks (ANN) have been used to fit the NMR FID data since the 1990s and have become very attractive recently.(Hansen, 2019; Hiltunen et al., 1995; Karunanithy and Hansen, 2021; Kern et al., 2020; Lee et al., 2020; Li et al., 2021, 2023) ANN has been used to fit the frequency domain chemical shift NMR data or other spectra with convoluted Gaussian or Lorentzian peaks. There are significant differences between wave and peak data fitting. The frequency domain peak fitting is to decouple overlapped peaks due to peak broadening, while the time domain FID fitting is to obtain the chemical shift peaks with corrected peak heights and phases. While pattern recognition of chemical shift peaks and direct analysis of FID seems feasible, neural networks require high-quality simulated data to mimic the complicated collection conditions in experiments.(Kern et al., 2020; Lee et al., 2020) In this report, we simulated FID data and analyzed them using both FFT and LSF methods as comparisons of their advantages.

2 Methods

All simulations and analyses are done using MATLAB R2024a on a Lenovo laptop with an Intel i7-13800H CPU and 32 GB of memory. Parallel computation using 4 cores is sometimes introduced to slightly speed up the simulations. The source code is available online at GitHub https://github.com/nkchenjx/jcNMR.

NMR FID signals are simulated using the chemical shifts of peaks. Three different peak shapes are used. (1) Single pure frequency with an exponential damping. (2) Peaks with Gaussian distributed frequencies with an exponential damping. (3) Peaks with Gaussian distributed frequencies that are broadening over time with an exponential damping. A summed chemical shift over all range of interests over time is constructed from these parameters, showing a damping chemical shift over time. The shift step is set to be 0.001 ppm, and the window is set to be -10 to 10 ppm to simulate ^{1}HNMR.

The frequencies of the peaks are calculated from the chemical shifts (δ ppm) of the peaks and the reference frequency f_{ref},

$$f_{\text{peak}}(\text{Hz}) = f_{\text{ref}}\delta_{\text{peak}} \times 10^{-6} + f_{\text{ref}} \qquad (1)$$

https://doi.org/10.5194/mr-2026-8
Preprint. Discussion started: 1 June 2026
© Author(s) 2026. CC BY 4.0 License.

Open Access MAGNETIC RESONANCE Discussions

e.g., for a reference frequency of TMS at f_{ref} = 500×10^6 Hz (default), and δ chemical shift (ppm), the frequency of an FID signal at a chemical shift δ_{peak} centered at 1 ppm will have a center frequency of 500,000,500 Hz.

The FID signal of each data point at time t is numerically simulated from stepwise frequencies using the following equation,

$$I(t) = \sum_{\text{peak}} \sum_f A_f e^{i(2\pi f t + \phi)} e^{-t/\tau} \qquad (2)$$

Where A_f is the amplitude of the signal at the frequency f, i is the imaginary unit $\sqrt{-1}$, ϕ is the initial phase shift, and τ is the lifetime of the damping of each peak. The spacing step of the numerical frequency summation is chosen to be significantly smaller than the width of the peak for reasonable convergence to integrations. This equation is a combination of damping cosine and sine wave functions in real and imaginary dimensions. Positive imaginary terms fix the rotation to be clockwise and use -i if one wants anticlockwise, or combine both if needed. The anticlockwise signal at 1 ppm after clockwise FFT will be mirrored with 0 ppm and show up at -1 ppm.

The time sequence is selected at a sampling step T_s such that the signal at the reference frequency is weak or invisible.

$$f_{\text{ref}} T_s = 2n\pi \qquad (3)$$

Where n is an arbitrary integer of choice, or a random duration with a filtration of the reference frequency. The default T_s is set to 0.0001 seconds and the number of data points is set to 2048 if not mentioned. The FID signal represents the difference between the frequency signal of a sample and the reference frequency because T_s is chosen (**Eq. 3**) to cancel the signal from the reference frequency (**Eq. 1**). i.e.,

$$I(t) = \sum_{peak} \sum_{\delta} A e^{i(2\pi f_{ref} \delta_{peak} \times 10^{-6} t + \phi) - t/\tau} \qquad (4)$$

Both time and signal noises are added to this signal to simulate an NMR measurement. The default time noise is 10 ps, and the default signal noise is set to be Gaussian with a standard deviation of 0.001.

Chemical shift peak broadening in the simulation window 0±10 ppm is simulated using a discrete Gaussian function,

$$y = \frac{A}{\sqrt{2\pi}\sigma} \Delta\delta e^{-\frac{(x-\delta_c)^2}{2\sigma^2}} \qquad (5)$$

Where A is the total peak area, assumed to be proportional to the concentration of the atoms in the molecule, σ is the standard deviation of the Gaussian peak, $\Delta\delta = 0.001$ (default) is the simulation step size of the chemical shift, x is the independent variable chemical shift with a step size $\Delta\delta$, and δ_c is the center of the Gaussian peak.

The broadening of the Gaussian peak width over time is simulated to be

$$\sigma_t = \sigma_0 + \sqrt{2Bt} \qquad (6)$$

Where σ_t and σ_0 are the standard deviation of the initial Gaussian chemical shift peaks at time t and zero, respectively, and B is the broadening rate, representing the effective diffusion coefficient with unit ppm^2/s, which is correlated with the true diffusion constant of the molecule in the solution.

The simulated FID time sequences are used in further analysis, including discrete Fast Fourier transformation (FFT) and least squares wave fitting. FFT converts simulated and experimental FID signals to chemical shift signals δ by,

$$f_k(\text{Hz}) = \sum_{n=1}^{N} I_n e^{-i2\pi f_k (n-1) T_s} \qquad (7)$$

https://doi.org/10.5194/mr-2026-8
Preprint. Discussion started: 1 June 2026
© Author(s) 2026. CC BY 4.0 License.

Open Access MAGNETIC RESONANCE Discussions

$$\delta_k(\text{ppm}) = \frac{f_k}{f_{ref}} \times 10^6 \qquad (8)$$

Where f_k is the k^{th} frequency of interest, n is the n^{th} FID data point in the time sequence with time interval T_s and the total number of data points N, I_n is the FID signal, i is the imaginary unit, and f_{ref} is the reference frequency in Hz.

The real and imaginary components of the signal carry phase information and are distorted in the frequency domain. These peaks have Lorentzian line shapes on top of their simulated Gaussian broadening. FFT of only real signals or only imaginary signals produces peaks with mirror chemical shifts of the signals with respect to 0 ppm. Thus, it could be better to use the complex signal for FFT.

Least squares wave fitting is done using a published algorithm JCFit, whose detailed procedure has been explained before.(Chen, 2024b, a, 2023) Briefly, each parameter in the wave damping model is scanned by simulation sequentially to find a fit to the simulated data with minimum sum squares of the residuals. The search sequence of the list of parameters is randomized at the beginning of each iteration.

Short-time Fourier transform (STFT), deep-learning STFT, and wavelet transform using simulated FID with 1024 data points. It simply places a selection window of the data points to run FFT and moves the window with fixed data points at a time. Piecewise data points from the FID time sequence are used to be convoluted with Fourier series or wavelet series with different frequencies to transform the 1D FID time domain data to 2D frequency domain spectra over discrete time, forming a spectrogram. An example of right-handed discrete wavelet transformation can be a 2d grid of frequency f and time t,

$$Wlt(f,t) = \sum_{x=t-\frac{w}{2}}^{t+\frac{w}{2}} FID(x) e^{-\frac{(x-t)^2}{2\sigma^2}} e^{i(2\pi f x - \phi)} \qquad (12)$$

where w is the convolution window of the Gaussian wavelet, σ is the standard deviation of the wavelet, i is the imaginary unit, x is the time sequence of the convolution window, and ϕ is the original phase shift. For comparison, window width w is set to 256 data points, and each time step is 36 data points with 220 data points overlapping between adjacent time windows. Please check the source code for details.

3 Results and Discussion

3.1 Comparing simulation methods

The actual collection of the FID signal during an experimental measurement is acquired at a time interval (T_s) of each data point with an acquisition time window (T_w, typically $T_w << T_s$), i.e., the continuous waves are sparsely sampled. However, simulating the collection window is computationally costly, especially for signals with complicated peaks. Thus, a point sampling of the actual signal is preferred to simulate a lot of FID spectra. The effect of different collection windows is tested. No apparent difference other than phase shift and amplitude variation is observed under conditions simulating an experimental setting (**Fig. 1**). This null effect is reasonable because integrating a sine or cosine wavefunction is a complementary cosine or sine function, respectively, with the same frequency signals but different phases and amplitudes.

https://doi.org/10.5194/mr-2026-8
Preprint. Discussion started: 1 June 2026
© Author(s) 2026. CC BY 4.0 License.

Open Access MAGNETIC RESONANCE Discussions

$$FID(t) = \int_{t}^{t+t_w} e^{i(2\pi f x - \phi)} dx =$$

$$\frac{1}{2\pi f i}[e^{i(2\pi f(t+t_w)-\phi)} - e^{i(2\pi f t-\phi)}] = Ae^{i\left(2\pi f t-\phi'-\frac{\pi}{2}\right)} \quad (9)$$

Where t is the time when the corrector starts working, t_w is a fixed-length-and-shape collection window, i is the imaginary unit $\sqrt{-1}$, f is the true frequency of the signal, ϕ is the starting phase constant of the signal at time zero, x is time, A is a new constant, and ϕ' is a new phase shift constant. This assumes that only the two side areas of the collection window contribute to the signal, and the middle part with full wave cycles is canceled. Thus, an ultra-sharp-edge rectangle collection window will give the same results as one-point data with phase and amplitude varied. A tunable edge slope and shape are simulated.

Fourier transform of the discrete FID signal regenerates a series of evenly distributed frequencies, including the original frequency,

$$\sum_{n=1}^{N} FID_n e^{-i2\pi f(n-1)T_s} = y[\left(f - f_{ref}\right) + \frac{l}{T_s}] \quad (10)$$

Where l = 1, 2, 3,… and y is the signal in the frequency domain. The set of frequencies f between f_{ref} to f_{ref}+1/T_s (Hz) is used in experimental practices to calculate the chemical shifts.

$$\delta_k(\text{ppm}) = \frac{f - f_{ref}}{f_{ref}} \times 10^6 \quad (11)$$

Typical NMR collection windows of an NMR machine are trapezoids whose effects are simulated. The onset timing, end timing, and the edge slopes all affect the phase shift. The edge slope affects the amplitude, and the sharper the better (**Fig. 1**). For example, 500 MHz ^{1}HNMR FID signals simulated using different methods are shown in **Fig. 1**. In addition to the amplitude noise determined by the FID collection precision, the quality of the signal is mainly determined by the accuracy of the starting time point and the repeatability of the collection window length. The time intervals are simulated to be <10 ps error in this example for >500 signal-to-noise ratio. The uniformity of magnification over the frequencies is correlated with the sharpness of the trapezoid's sides. In these simulations, a sharp <1 ns ramp time is needed for uniform amplification of signals for the chemical shifts of interest (0-10 ppm). As a reference, a 500 MHz rotational signal has a 2 ns wave cycle time.

https://doi.org/10.5194/mr-2026-8
Preprint. Discussion started: 1 June 2026
© Author(s) 2026. CC BY 4.0 License.

Open Access MAGNETIC RESONANCE Discussions

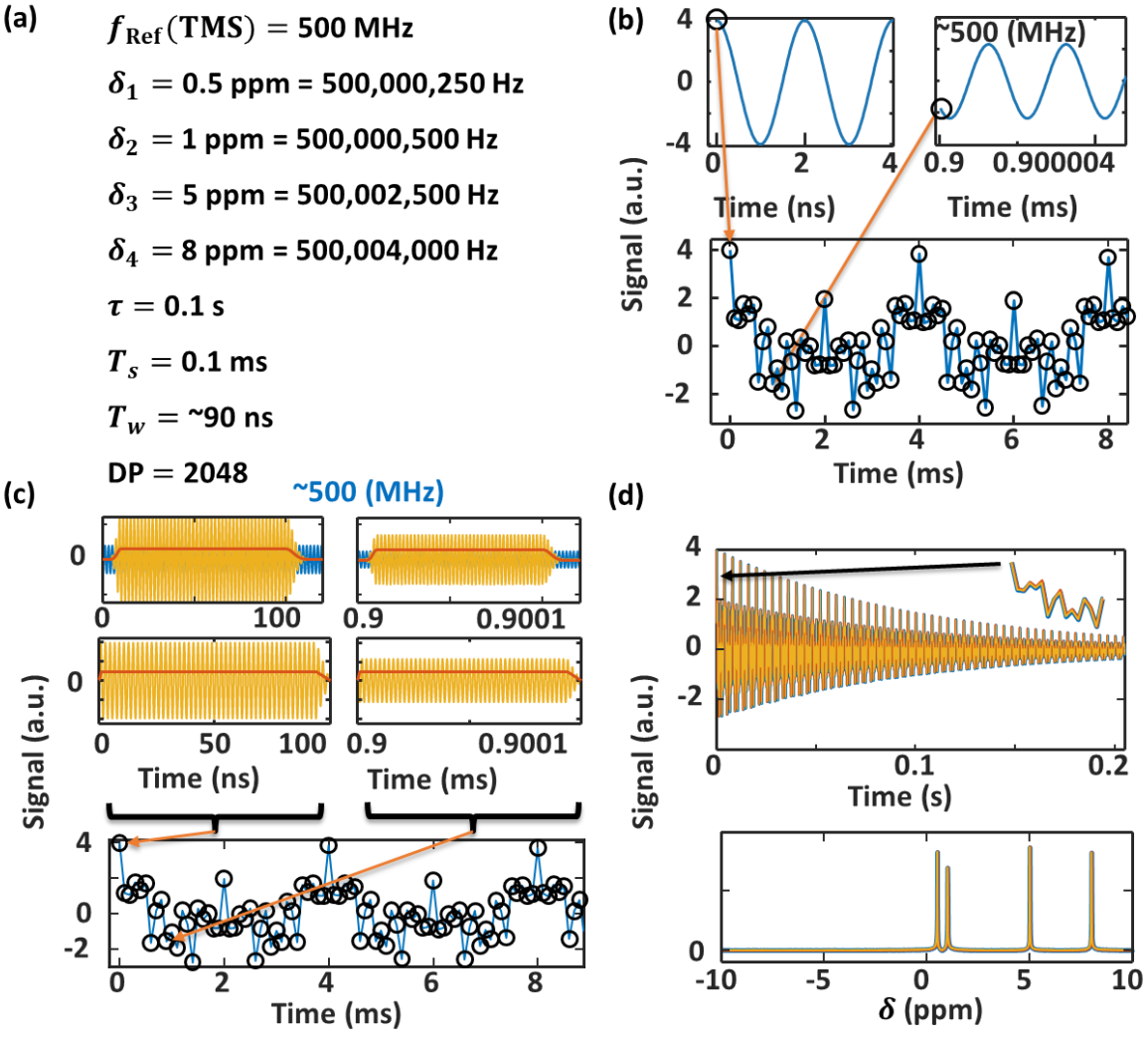

Figure 1: Simulating the effect of NMR data collecting parameters. (a) Simulation parameters of a ^{1}HNMR FID signal with four frequencies, each having amplitude 1, phase shift 0 at time zero, and 0.1 s damping lifetime. (b) Scheme of using the initial combined signal at each time point as the FID signal. (c) Scheme of using the accumulated signal (summation) in each window as the signal. Two collection windows, one with Gaussian sides and the other with linear sides, are shown to have the same FID signal as in (b) after magnification and phase shifting. (d) Three FID simulations from (b, c) and their chemical shift peaks after FFT overlap with negligible differences after phase correction.

Thus, the single-point value of the wave function at time t is used to simulate the FID signal instead of the integration of the wave signal in the correction window t to $t+t_w$. The signal loss and phase shift due to collection windows can be simulated by tuning the amplitude and phase of the wave function. No obvious difference between simulations of one-point data collection and 90-ns data collection is observed, so one-point data collection is used in the following simulations. This choice significantly improves the simulation cost-efficiency.

https://doi.org/10.5194/mr-2026-8
Preprint. Discussion started: 1 June 2026
© Author(s) 2026. CC BY 4.0 License.

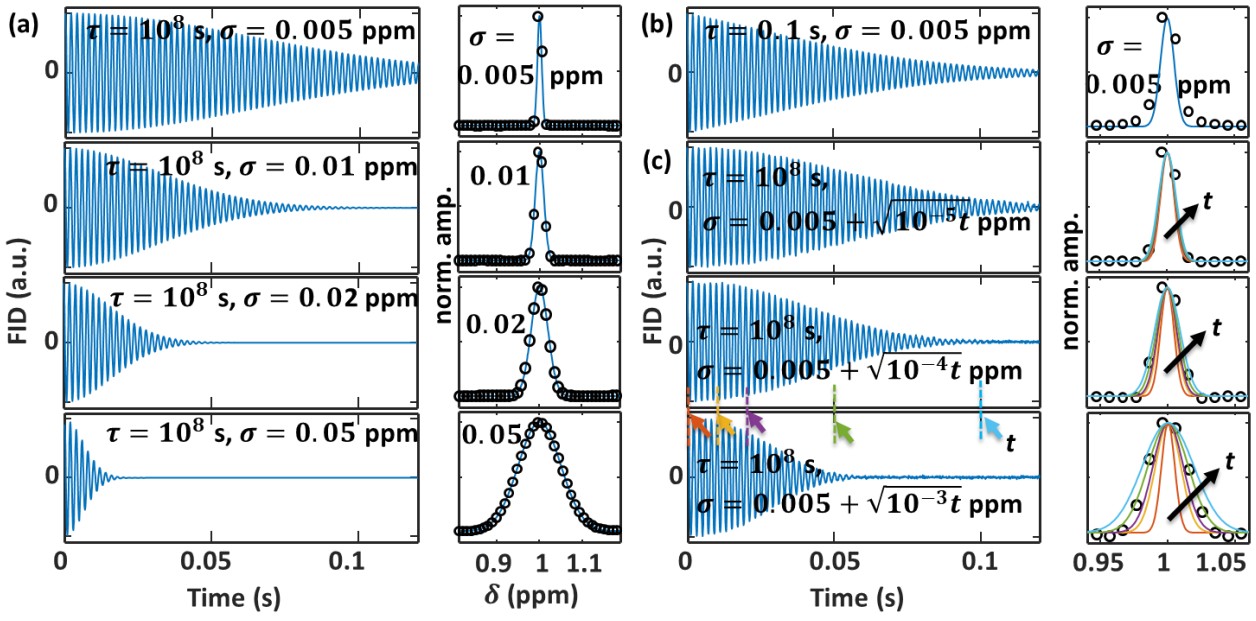

Figure 2. Simulated FIDs with chemical shift peak Gaussian broadened and their FFT peaks. TMS 500 MHz, $\delta = 1$ ppm with simulation resolution at step size 0.001 ppm, $T_s = 0.1$ ms, data points 2048 one-point collection, and the rest of the parameters are shown in the figure. (a) No damping, only different Gaussian broadening for comparison. The Gaussian peaks for simulation are normalized by height with the overlay circles representing the normalized FFT results. (b) Adjusting the damping lifetime to have a comparable effect on the FID decay rate as the Gaussian peak broadens. (c) The effect on the FID decay of Gaussian peaks evolving broader over time.

FID signal of chemical shifts with Gaussian broadening and diffusion is then simulated (**Fig. 2**). Once a fixed peak broadening over time is introduced, both dephasing (interference) and damping control the decay speed of the FID signals (**Fig. 2a, 2b**). For each chemical shift peak, many signals with slightly broadened frequencies are first synchronized in phase, and then they decay due to damping. They also start to lose phase synchronization over time, and the signal cancels out due to interference. Thus, the FID signal with measurable amplitude is significantly shortened, dominated by the dephasing of the signals when the damping is negligibly small with a very large decay lifetime e.g. 10^8 s, ~3 years. (**Fig. 2a**). Peaks further apart in chemical shifts usually do not interfere with each other.

When a comparable damping lifetime is introduced, e.g. 0.1 s in **Fig. 2b**, the FID decays faster than no damping. Damping also adds additional broadening to FFT peaks. At this damping rate, the real part of the FFT signals with proper phase corrections has peaks slightly broader than the true values (**Fig. 2b**).

When the Gaussian chemical shift peaks are simulated to be dynamic and further broaden over time, the FID signal decays faster than the fixed-width Gaussian peak simulations due to the dephasing increases with the further broadening over time (**Fig. 2c**). When the damping is set to be negligible to simplify comparison, the real part of the FFT peak is consistent with the

https://doi.org/10.5194/mr-2026-8
Preprint. Discussion started: 1 June 2026
© Author(s) 2026. CC BY 4.0 License.

Open Access MAGNETIC RESONANCE Discussions

Gaussian peak width of the latter tail part of the FID signal with measurable amplitude. This consistency is expected because FFT reflects the average peak width of the useful signals.

Simulating 1,000 random FIDs each with 1024 data points and tens of randomly evolving Gaussian chemical shift peaks with 0.001 ppm resolution takes ~1 hour, for a single CPU of a typical laptop or desktop with an Intel i7 CPU. Parallel computation using multiple CPUs or GPUs can significantly speed up such batch simulations.

3.2 NMR FID signal least squares regression fitting

The Jump-Chain Fitting (JCFit) algorithm we developed can fit FID using the initial guess obtained from the FFT results. For an example simulation of chemical shifts with fixed Gaussian width over time (**Fig. 3a**), JCFit using the simplest model, damping single frequency (no width, no broadening, and no initial phase shift) with initial guesses from the FFT results, can fit the FID with reasonable initial amplitudes with $R^2 = 0.99$ (**Fig. 3b**). The amplitudes are similar to the FFT results, yet FFT is orders of magnitude faster than JCFit. Because no peak width and dephasing are fitted, the damping rates are off the true values. Initial phase shifts if simulated, can be correctly fitted. If the same model with wave interferences as the simulation is used during the fitting, JCFit has the potential to fit the parameters but will be unacceptably slow.

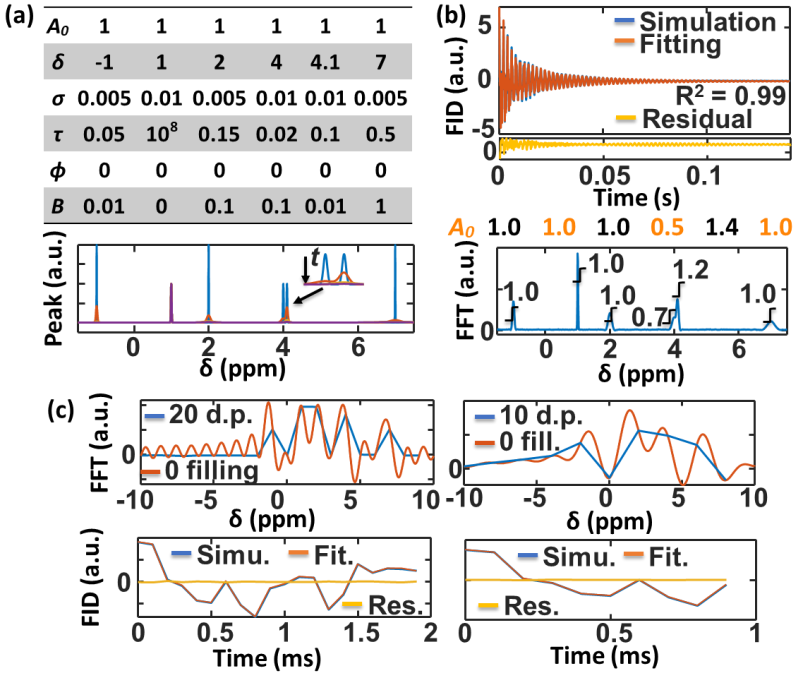

Figure 3: Least squares fitting of FID. (a) Simulation parameters of 500 MHz ^{1}HNMR. (b) Least squares fitting of simulated 2048 data point FID using single frequency; fitted A_0; and real part of the FFT of FID with integrated area shown with error <±0.1 ppm except for the doublets at 4 ppm. (c) Simulations with 20 and 10 data points using the same parameters, adding some random initial phase shifts. The real part of FFTs, and the least squares fitting of the FID data are shown, which still yield an accuracy of chemical shift within 0.1 ppm except for the peaks at 4 ppm. 20 data points (500 Hz) are about one wave cycle of the peak at chemical shift ~1 ppm.

https://doi.org/10.5194/mr-2026-8
Preprint. Discussion started: 1 June 2026
© Author(s) 2026. CC BY 4.0 License.

Open Access MAGNETIC RESONANCE Discussions

A significant advantage of fitting over FFT can be seen in very short data. JCFit is fast and promising to fit very few data points when FFT has difficulties, e.g., it takes a few seconds to fit 20 or 10 data points that are shorter than the wave cycle of the slowest frequency (21 data points for $\delta = 1$ ppm). FFT struggles to obtain enough resolution for data shorter than one cycle. The FFT of data with or without 0s added after the data to 2048 data points, is significantly less accurate than the FFT of longer data (**Fig. 3c**). Zero filling is a commonly used method to improve the frequency resolution of FFT.(Comisarow and Melka, 1979) The least squares fitted chemical shift and amplitude are similar to those obtained from the long data, correctly fitted amplitude and shift of all peaks within 1% error (**Fig. 3c**), except that the amplitudes of the doublets at 4 ppm cannot be correctly resolved similar to the FFT and fitting of the longer data. And the fit of these two peaks has a relatively large error of the shift ~0.2 ppm. Nevertheless, the fitted results are much better than FFT for this simple signal, providing comparable accuracy with much longer data. Fitting will be very challenging for complicated molecules.

3.3 Short-time Fourier transformation, wavelet, and machine learning

FFT is sensitive to data length but does not need the whole FID signal for high-resolution frequency transformation. Short-time Fourier transformation (STFT) and wavelet transformation (WT) are natural extensions of the FID data analysis and have shown potential in NMR tuning.(Hirakawa et al., 2019; Kim et al., 2015; Liu et al., 2016) STFT breaks the FID into pieces or uses a moving window to select the subsets of data for FFT analysis with/without zero filling and plots the frequency signals in a time sequence, which can be used to construct a frequency-time spectrogram. For example, apply FFT to FID data at 0-0.02, 0.01-0.03 s, etc, with a 20 ms time window. Spectrograms are commonly used for machine learning, such as sound pattern characterization. The piecewise FID signal decouples some peaks with different decay lifetimes, and the short sequence contains less random noise. Both destructive and constructive interference among peaks are observed. Wavelet transformation uses a similar idea but directly applies wave packets to move through the FID signals to extract the frequency signal that matches the wave packets' frequencies. It usually uses a shaped wave instead of a rectangular wave in the FFT. For example, moving convolution Gaussian wavelet with frequencies 1, 2, … Hz to the FID data over time. Deep learning STFT (DLSTFT) constructs piecewise frequency peaks for neural network training.

Short-time Fourier transform (STFT) of FID offers a dynamic view of the decay of frequencies over time and their interferences. **Fig. 4** shows a comparison of FFT and piecewise short-time FT methods in analyzing simulated ^{1}HNMR FID signals. STFT, DLSTFT, and wavelet Fourier transform show similar dynamics of the chemical peak decay with dephasing and interference effects. All three methods reduce the frequency resolution compared to FFT as expected. These methods use shorter pieces while FFT uses the whole FID data set. STFT offers the best peak resolution using sharp-edged convolution wave windows. Gaussian wavelet FT using wave packets has "softer" window edges and shorter effective window sizes, thus, its frequency resolution is poorer than STFT with a similar window size. Wavelet has a possible advantage in less edge effect

https://doi.org/10.5194/mr-2026-8
Preprint. Discussion started: 1 June 2026
© Author(s) 2026. CC BY 4.0 License.

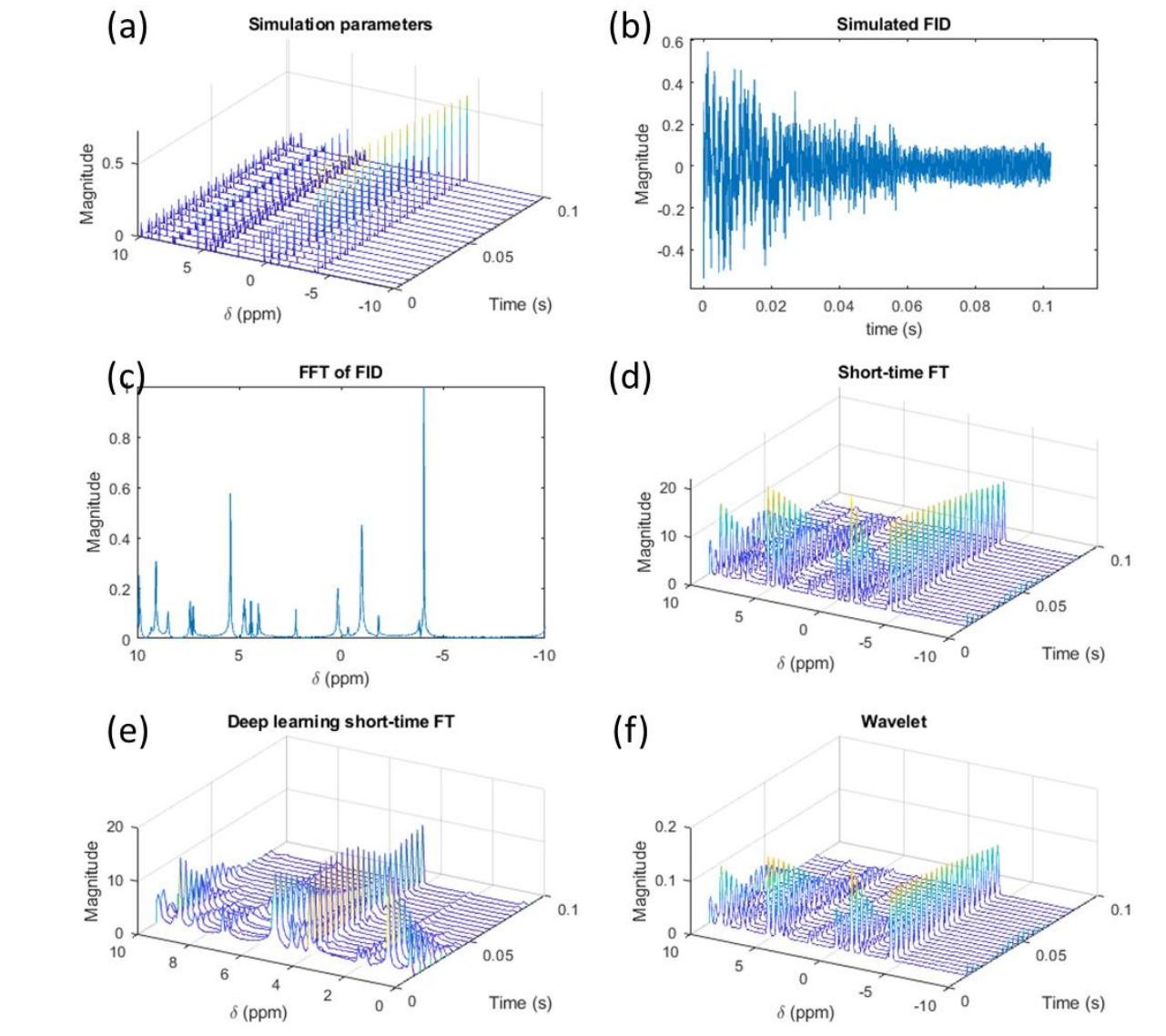

Figure 4: An example of 10,000 randomly simulated ^{1}HNMR and analysis results. (a) Gaussian chemical shift peaks damping over time with no further broadening. (b) The real part of the simulated FID. Absolute values of (c) FFT, (d) STFT (~0.02 s data per time step), (e) DLSTFT from MATLAB does not support complex input, so peaks are mirrored over the reference shift at zero, and (f) wavelet analysis of the simulated FID signals.

215

https://doi.org/10.5194/mr-2026-8
Preprint. Discussion started: 1 June 2026
© Author(s) 2026. CC BY 4.0 License.

Open Access MAGNETIC RESONANCE Discussions

4 Conclusion

This report compares several simulation methods for Nuclear Magnetic Resonance (NMR) free induction decay (FID) signals and various data analysis techniques to transform FID from the time domain to the frequency domain. The methods discussed include fast Fourier transform (FFT), direct fitting, and piecewise Fourier transform.

Chemical shift peak frequencies can be used to simulate FID signals at collection time steps with intervals much longer than the wave cycles. However, simulating the broadening of these peaks reveals that the interference of different parts of the peak dampens the intensity of the FID signal and cannot be ignored. Therefore, the starting point signal of the data collection time step for each frequency is summed to obtain the apparent FID data point. The simulation frequency resolution should be much finer than the peak width of the chemical shifts.

Ideally, integrating the convolution of the collection window with the hidden FID signals would simulate the experimental data collection process, but this is computationally expensive. If the collection window edge is sharp enough, its effect can be relatively small.

FFT offers a very fast and accurate transformation of time domain FID signals to frequency domain peak shift signals. When the length of data points is short and even compatible with or shorter than one wave cycle, zero fillings are added to get enough data points for FFT to work. However, the resolution and accuracy significantly drop due to the small fraction of useful signals. For these short data, direct wave fitting using methods such as least-squares fitting has advantages but is challenging because the error space of wave fitting has a wave-like local minima structure, which is easy to get stuck in. The recently developed jump-chain random searching algorithm searches larger spaces in each iteration, making it better than the gradient descent method at overcoming local minima. Although it is very slow for long FID signals, it is suitable for fitting very short FID pieces to extract major peaks. Fitting can work for simple molecules with few peaks, but it is challenging for complex molecules, when inverse Fourier transform may be useful to extract the signals of different frequency regions.

Deep learning analysis of FID signals requires high-quality spectrograms. Simulated data are needed to prepare the training library for chemicals collected using different NMR machines and data collection conditions. The current comparison shows that STFT offers good frequency resolution in generating spectrograms from FID data. For FID with mixed chemicals, a potential challenge can be the complicated interference patterns on the spectrograms among peaks from different compounds. Nevertheless, using STFT, DLSTFT, or wavelet spectrograms to train artificial neural networks that can quickly classify chemicals is a promising future pursuit, analogous to classifying human speech.

Code and data availability

The source code of JCFit in MATLAB is also available on GitHub https://github.com/nkchenjx/JCFit. The source code for generating the figures in this report is available at GitHub https://github.com/nkchenjx/jcNMR.

https://doi.org/10.5194/mr-2026-8
Preprint. Discussion started: 1 June 2026
© Author(s) 2026. CC BY 4.0 License.

Open Access MAGNETIC RESONANCE Discussions

Author contributions

JC developed the model code, performed the simulations, and wrote the manuscript.

Competing interests

The author declares no competing financial interest.

Disclaimer

Copernicus Publications remains neutral with regard to jurisdictional claims made in the text, published maps, institutional affiliations, or any other geographical representation in this paper. While Copernicus Publications makes every effort to include appropriate place names, the final responsibility lies with the authors. Views expressed in the text are those of the authors and do not necessarily reflect the views of the publisher.

Acknowledgements

Chen thanks Prof. Edward Saliba for constructive comments and discussion. Chen thanks Prof. Robert Hamers for his mentorship and for introducing the Fourier transform during his postdoctoral training at the University of Wisconsin-Madison, particularly in the context of various optical and electronic spectroscopic techniques. Chen thanks Ohio University Nanoscale and Quantum Phenomena Institute.

Financial support

National Human Genome Research Institute (NHGRI) at the National Institutes of Health (NIH), USA, award number 2R15HG009972. The content is solely the responsibility of the authors and does not necessarily reflect the official views of NHGRI.

https://doi.org/10.5194/mr-2026-8
Preprint. Discussion started: 1 June 2026
© Author(s) 2026. CC BY 4.0 License.

Open Access MAGNETIC RESONANCE Discussions

References

van Beek, J. D.: matNMR: A flexible toolbox for processing, analyzing and visualizing magnetic resonance data in Matlab®, Journal of Magnetic Resonance, 187, 19–26, https://doi.org/10.1016/j.jmr.2007.03.017, 2007.

Bothner-By, A. A. and Naar-Colin, C.: The Proton Magnetic Resonance Spectra of 2,3-Disubstituted *n* -Butanes, J. Am. Chem. Soc., 84, 743–747, https://doi.org/10.1021/ja00864a013, 1962.

Castellano, S. and Bothner-By, A. A.: Analysis of NMR Spectra by Least Squares, The Journal of Chemical Physics, 41, 3863–3869, https://doi.org/10.1063/1.1725826, 1964.

Chen, J.: nkchenjx/pyjcfit, 2023.

Chen, J.: nkchenjx/jcfit, 2024a.

Chen, J.: Structured stochastic curve fitting without gradient calculation, Journal of Computational Mathematics and Data Science, 12, 100097, https://doi.org/10.1016/j.jcmds.2024.100097, 2024b.

Comisarow, M. B. and Melka, J. D.: Error estimates for finite zero-filling in Fourier transform spectrometry, Anal. Chem., 51, 2198–2203, https://doi.org/10.1021/ac50049a032, 1979.

Esvan, Y. J. and Zeinyeh, W.: Basics of Fourier Transform Applied to NMR Spectroscopy: An Interactive Open-Source Web Application, J. Chem. Educ., 97, 263–264, https://doi.org/10.1021/acs.jchemed.9b00502, 2020.

Hagaman, E. W., Hoch, J. C., and Stern, A. S.: NMR Data Processing, Radiation Research, 147, 272, https://doi.org/10.2307/3579432, 1997.

Hamers, R., Hayes, S., and Peaslee, G.: Mid-Scale Instrumentation: Regional Facilities to Address Grand Challenges in Chemistry, Chemistry Faculty Publications, https://doi.org/10.7936/K71G0KF7, 2017.

Hansen, D. F.: Using Deep Neural Networks to Reconstruct Non-uniformly Sampled NMR Spectra, Journal of Biomolecular NMR, 73, 577–585, https://doi.org/10.1007/s10858-019-00265-1, 2019.

Hiltunen, Y., Heiniemi, E., and Alakorpela, M.: Lipoprotein-Lipid Quantification by Neural-Network Analysis of 1H-NMR Data from Human Blood Plasma, Journal of Magnetic Resonance, Series B, 106, 191–194, https://doi.org/10.1006/jmrb.1995.1032, 1995.

Hirakawa, K., Koike, K., Kanawaku, Y., Moriyama, T., Sato, N., Suzuki, T., Furihata, K., and Ohno, Y.: Short-time Fourier Transform of Free Induction Decays for the Analysis of Serum Using Proton Nuclear Magnetic Resonance, Journal of Oleo Science, 68, 369–378, https://doi.org/10.5650/jos.ess18212, 2019.

Hulse, S. G.: Estimation of NMR signals in the time domain: methodology, applications and software, PhD thesis, University of Oxford, 2023.

Kalstabakken, K. A. and Harned, A. M.: Spectral Database for Instructors: A Living, Online NMR FID Database, J. Chem. Educ., 90, 941–943, https://doi.org/10.1021/ed300787v, 2013.

Karunanithy, G. and Hansen, D. F.: FID-Net: A versatile deep neural network architecture for NMR spectral reconstruction and virtual decoupling, Journal of Biomolecular NMR, 75, 179–191, https://doi.org/10.1007/s10858-021-00366-w, 2021.

https://doi.org/10.5194/mr-2026-8
Preprint. Discussion started: 1 June 2026
© Author(s) 2026. CC BY 4.0 License.

Open Access MAGNETIC RESONANCE Discussions

Kern, S., Liehr, S., Wander, L., Bornemann-Pfeiffer, M., Müller, S., Maiwald, M., and Kowarik, S.: Artificial neural networks for quantitative online NMR spectroscopy, Analytical and Bioanalytical Chemistry, 412, 4447–4459, https://doi.org/10.1007/s00216-020-02687-5, 2020.

Kim, B., Kong, S.-H., and Kim, S.: Low Computational Enhancement of STFT-Based Parameter Estimation, IEEE Journal of Selected Topics in Signal Processing, 9, 1610–1619, https://doi.org/10.1109/JSTSP.2015.2465310, 2015.

Lee, H., Lee, H. H., and Kim, H.: Reconstruction of spectra from truncated free induction decays by deep learning in proton magnetic resonance spectroscopy, Magnetic Resonance in Medicine, 84, 559–568, https://doi.org/10.1002/mrm.28164, 2020.

Li, D.-W., Hansen, A. L., Yuan, C., Bruschweiler-Li, L., and Brüschweiler, R.: DEEP picker is a deep neural network for accurate deconvolution of complex two-dimensional NMR spectra, Nature Communications, 12, 5229, https://doi.org/10.1038/s41467-021-25496-5, 2021.

Li, D.-W., Bruschweiler-Li, L., Hansen, A. L., and Brüschweiler, R.: DEEP Picker1D and Voigt Fitter1D: a versatile tool set for the automated quantitative spectral deconvolution of complex 1D-NMR spectra, Magn. Reson., 4, 19–26, https://doi.org/10.5194/mr-4-19-2023, 2023.

Liu, H., Dong, H., Ge, J., Bai, B., Yuan, Z., and Zhao, Z.: Research on a secondary tuning algorithm based on SVD & STFT for FID signal, Meas. Sci. Technol., 27, 105006, https://doi.org/10.1088/0957-0233/27/10/105006, 2016.

Montigny, F., Brondeau, J., and Canet, D.: Analysis of time-domain NMR data by standard non-linear least-squares, Chemical Physics Letters, 170, 175–180, https://doi.org/10.1016/0009-2614(90)87111-4, 1990.

Nicolay, K., Braun, K. P. J., Graaf, R. A. de, Dijkhuizen, R. M., and Kruiskamp, M. J.: Diffusion NMR spectroscopy, NMR in Biomedicine, 14, 94–111, https://doi.org/10.1002/nbm.686, 2001.

Nishiyama, K. and Mita, T.: High resolution NMR spectroscopy using a recursive algorithm, IEEE Trans. Biomed. Eng., 36, 222–231, https://doi.org/10.1109/10.16469, 1989.

Orekhov, V., Kasprzak, P., and Kazimierczuk, K.: Data Processing Methods: Fourier and Beyond, in: Two-Dimensional (2D) NMR Methods, 19–46, https://doi.org/10.1002/9781119806721.ch2, 2023.

Sacristán-Martín, A., Álvarez-Llorente, N., Diez-Varga, A., Barbero, H., and Álvarez, C. M.: Ru(II)-Based Multitopic Hosts for Fullerene Binding: Impact of the Anion in the Recognition Process, Inorg. Chem., 64, 2360–2370, https://doi.org/10.1021/acs.inorgchem.4c04608, 2025.

Stern, A. S., Donoho, D. L., and Hoch, J. C.: NMR data processing using iterative thresholding and minimum l1-norm reconstruction, Journal of Magnetic Resonance, 188, 295–300, https://doi.org/10.1016/j.jmr.2007.07.008, 2007.

Vanhuffel, S., Chen, H., Decanniere, C., and Vanhecke, P.: Algorithm for Time-Domain NMR Data Fitting Based on Total Least Squares, Journal of Magnetic Resonance, Series A, 110, 228–237, https://doi.org/10.1006/jmra.1994.1209, 1994.

Weidkamp, K. P., Afzali, A., Tromp, R. M., and Hamers, R. J.: A Photopatternable Pentacene Precursor for Use in Organic Thin-Film Transistors, J. Am. Chem. Soc., 126, 12740–12741, https://doi.org/10.1021/ja045228r, 2004.

Wu, Y., Sanati, O., Uchimiya, M., Krishnamurthy, K., Wedell, J., Hoch, J. C., Edison, A. S., and Delaglio, F.: SAND: Automated Time-Domain Modeling of NMR Spectra Applied to Metabolite Quantification, Anal. Chem., 96, 1843–1851, https://doi.org/10.1021/acs.analchem.3c03078, 2024.

https://doi.org/10.5194/mr-2026-8
Preprint. Discussion started: 1 June 2026
© Author(s) 2026. CC BY 4.0 License.

Open Access MAGNETIC RESONANCE Discussions

Zhang, L., Zhu, D., Nathanson, G. M., and Hamers, R. J.: Selective Photoelectrochemical Reduction of Aqueous CO_2 to CO by Solvated Electrons, Angewandte Chemie, 126, 9904–9908, https://doi.org/10.1002/ange.201404328, 2014.